THE JOURNAL OF BIOLOGICAL CHEMISTRY VOL. 288, NO. 15, pp. 10759–10765, April 12, 2013

Ion Pathways in the Sarcoplasmic Reticulum Ca^{2+}-ATPase*

Published, JBC Papers in Press, February 11, 2013, DOI 10.1074/jbc.R112.436550

Maike Bublitz[‡§1], Maria Musgaard[‡¶2], Hanne Poulsen[‡§], Lea Thøgersen[‡‖], Claus Olesen[‡], Birgit Schiøtt[¶‡‡§§], J. Preben Morth[‡§3], Jesper Vuust Møller[‡**], and Poul Nissen[‡§]**

*From the [‡]Centre for Membrane Pumps in Cells and Disease (PUMPkin) and the [‡‡]Centre for Insoluble Protein Structures, Danish National Research Foundation, the Departments of [§]Molecular Biology and Genetics, [¶]Chemistry, and **Physiology and Biophysics, the [‖]Bioinformatics Research Centre, and the [§§]Interdisciplinary Nanoscience Center, Aarhus University, DK-8000 Aarhus C, Denmark*

The sarco/endoplasmic reticulum Ca^{2+}-ATPase (SERCA) is a transmembrane ion transporter belonging to the P_{II}-type ATPase family. It performs the vital task of re-sequestering cytoplasmic Ca^{2+} to the sarco/endoplasmic reticulum store, thereby also terminating Ca^{2+}-induced signaling such as in muscle contraction. This minireview focuses on the transport pathways of Ca^{2+} and H^+ ions across the lipid bilayer through SERCA. The ion-binding sites of SERCA are accessible from either the cytoplasm or the sarco/endoplasmic reticulum lumen, and the Ca^{2+} entry and exit channels are both formed mainly by rearrangements of four N-terminal transmembrane α-helices. Recent improvements in the resolution of the crystal structures of rabbit SERCA1a have revealed a hydrated pathway in the C-terminal transmembrane region leading from the ion-binding sites to the cytosol. A comparison of different SERCA conformations reveals that this C-terminal pathway is exclusive to Ca^{2+}-free *E*2 states, suggesting that it may play a functional role in proton release from the ion-binding sites. This is in agreement with molecular dynamics simulations and mutational studies and is in striking analogy to a similar pathway recently described for the related sodium pump. We therefore suggest a model for the ion exchange mechanism in P_{II}-ATPases including not one, but two cytoplasmic pathways working in concert.

P-type ATPases form a large family of transmembrane transporters that couple the energy from ATP hydrolysis to active transport of key cations across biological membranes. These so-called ion pumps are multidomain enzymes that contain polar and charged residues within their transmembrane (TM)[4] domain that mediate binding of the transported ions. For the most well studied members, the sarco/endoplasmic reticulum Ca^{2+}-ATPase (SERCA) and the Na^+/K^+-ATPase (NKA), the binding sites have been thoroughly described by structural and mutational studies (1–5), whereas the inherently dynamic interactions along the routes of ion entry and exit remain less clear.

P-type ATPases generally function according to an alternating access model (6–8) (also described as an *E*1/*E*2 scheme (9–11)) in which the ion-binding sites are accessible from either the cytoplasmic or extracytoplasmic side, interspersed by occluded states coupled with phosphorylation or dephosphorylation (12–14). Therefore, there must be at least one ion access pathway at each side of the membrane, but it has also been suggested that the Ca^{2+} exit and proton entry pathways on the luminal side of SERCA are separate (15). This article provides a focused review of the ion pathways in SERCA, pointing in particular to the possibility of two cytoplasmic pathways, one for proton exit and another for Ca^{2+} binding.

The Luminal/Extracellular Pathway: The "Exit Path"

The structure of SERCA in the *E*2P conformation (trapped as a phosphoenzyme intermediate mimicked by BeF_3^-) revealed a luminal Ca^{2+} exit pathway (Exit path) (Fig. 1*a*) encompassed by TM segments M1–M6 (16, 17). This structure follows a conformational change in the *E*1P state upon completion of the phosphorylation reaction. Relaxation of the tense *E*1P conformation allows ADP release and a large rotation/translation of the A-domain, which then interacts with the phosphorylated P-domain. The *E*1P-to-*E*2P transition transduces into a spreading of the M1-M2 and M3-M4 segments away from the M5-M6 segment, which remains associated with the M7–M10 helix bundle. The geometry of the two Ca^{2+}-binding sites gets distorted by these movements, and three of the Ca^{2+}-coordinating residues (Glu^{309}, Glu^{771}, and Asn^{796}) are exposed to the luminal environment through a wide open, funnel-shaped exit pathway paved with polar side chains. A Mg^{2+} ion is bound at the exposed site, involving the otherwise Ca^{2+}-coordinating Glu^{309} and a second acidic residue, Glu^{90} (16). The effect of mutating Glu^{90} to alanine or leucine is a marked reduction in the apparent affinity for luminal Ca^{2+}, suggesting a direct interaction (18). If a permanent positive charge is introduced by an E90R mutation, the rate of dephosphorylation (the step that follows Ca^{2+} release and occlusion of H^+ during the pumping cycle) is reduced, and accordingly, the site has been described as a transient, low affinity Ca^{2+}-"leaving site" (18).

The recently reported *E*2P structure of porcine NKA in a high affinity complex with the cardiotonic steroid ouabain (19) displays a close analogy to the *E*2-BeF_3^- structure of SERCA.

* This work was supported by the European Union FP7 Program EDICT and the Danish Research Council Program DANSCATT, a postdoctoral fellowship from the Danish Medical Research Council (to C. O.), a Carlsberg fellowship (to J. P. M.), an Eliteforsk travel stipend from the Danish Research Council (to M. M.), and a Hallas-Møller stipend from the Novo-Nordisk Foundation and the European Research Council Advanced Research Program BIOMEMOS (to P. N.). This article is part of the Thematic Minireview Series on the Ins and Outs of Calcium Transport.

[1] To whom correspondence should be addressed. E-mail: mbu@mb.au.dk.

[2] Present address: Structural Bioinformatics and Computational Biochemistry, Dept. of Biochemistry, University of Oxford, Oxford OX1 3QU, United Kingdom.

[3] Present address: Centre for Molecular Medicine, Nordic EMBL Partnership, University of Oslo, N-0318 Oslo, Norway.

[4] The abbreviations used are: TM, transmembrane; SERCA, sarco/endoplasmic reticulum Ca^{2+}-ATPase; NKA, Na^+/K^+-ATPase; SPCA, secretory pathway Ca^{2+}-ATPase; MD, molecular dynamics; AMPPCP, adenosine 5′-(β,γ-methylene)triphosphate.

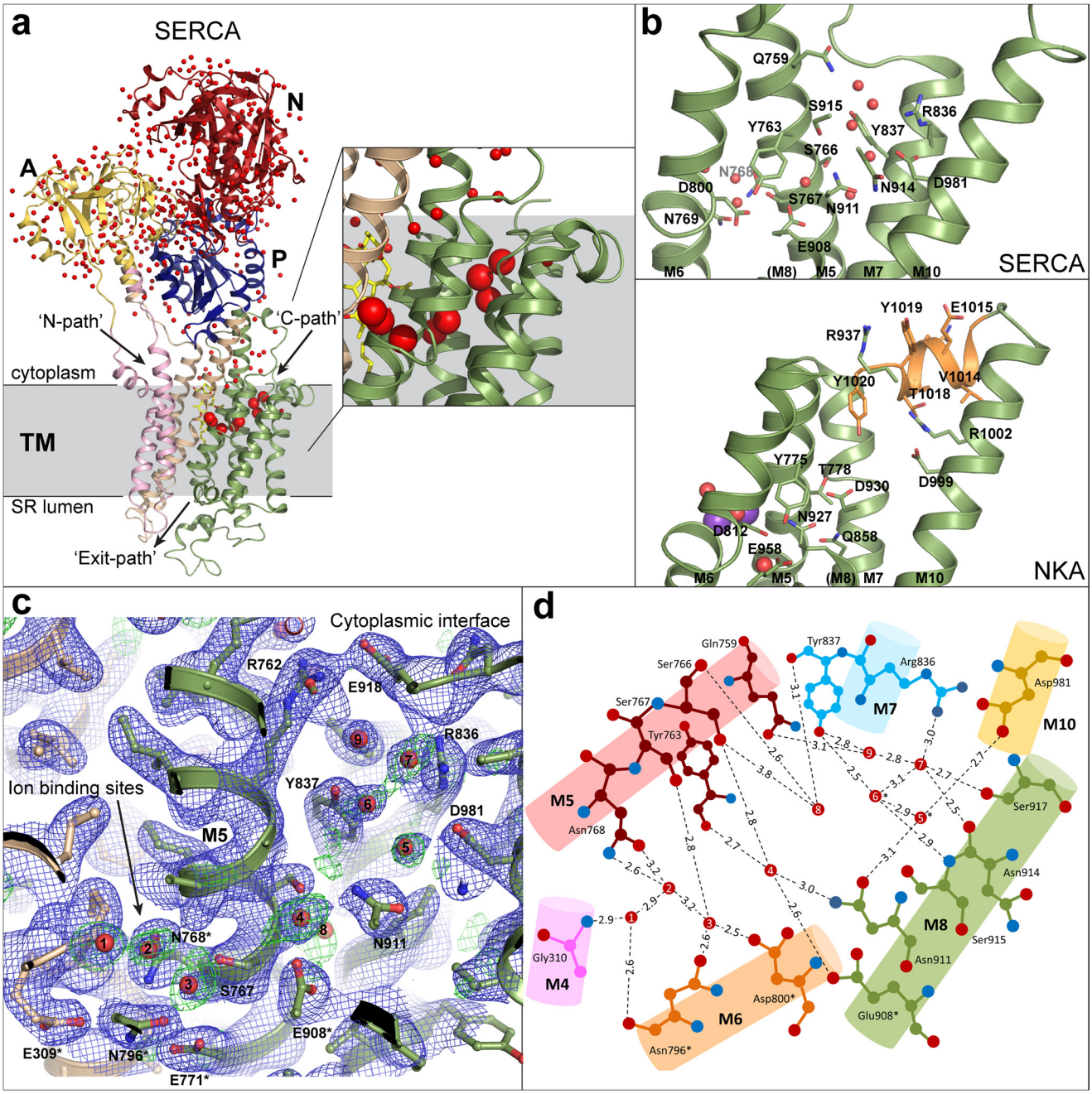

FIGURE 1. **Ion pathways in SERCA1a.** *a*, overall schematic representation of SERCA1a (Protein Data Bank code 3N5K), with bound water as *red spheres*. Domains are labeled as follows. *N*,: nucleotide-binding domain (*red*); *P*, phosphorylation domain (*blue*); *A*, actuator domain (*yellow*); *TM*, transmembrane domain, with M1-M2 in *pink*, M3-M4 in *beige*, and M5–M10 in *green*. The N-path, C-path, and Exit path are indicated by *arrows*. *Spheres* that represent waters inside the channel are scaled according to their van der Waals radius; all other waters are scaled to half-size. Thapsigargin is depicted as *yellow sticks*. A magnification of the C-path area is *boxed*. *b*, C-path of SERCA and NKA (code 2ZXE (38)), with polar and charged side chains shown as *sticks*, water molecules shown as *red spheres*, K^+ ions shown as *purple spheres*. The C-terminal extension in NKA is colored *orange*. NKA residue numbering is adapted to the human $\alpha 2$ sequence. *c*, experimental evidence for water molecules between helices M5, M7, M8, and M10. *Blue mesh*, $2F_o - F_c$ electron density map contoured at 1.0σ; *green mesh*, unbiased $F_o - F_c$ map contoured at 2.8σ. Polar residues lining the cavity and the ion-binding site are indicated. *d*, plot representation of the water network in the C-path and the residues interacting with the water molecules.

Although the Exit path is obstructed by ouabain in this structure, it suggests that the pathway is a conserved feature between the two pumps. Based on the two outward open structures, the Exit path is not only an exit pathway for Ca^{2+} or Na^+, but is also the entry pathway for the countertransported cations: H^+ for SERCA and K^+ for NKA. The Mg^{2+} ion stabilizing the open *E*2P state (16, 20) would therefore at the same time modulate the ion exchange kinetics.

Cytoplasmic Pathway I: The "N-path"

The very first structure of SERCA representing a nucleotide-free, Ca^{2+}-bound, *E*1-like state (4) shows a hydrophilic environment at the Ca^{2+}-binding sites, which are surrounded by straight helices M1, M2, M4, and M6, including unwound parts of M4 (^{309}EGLP^{312}) and M6 (^{800}DG^{801}) exposed to the cytoplasm. This structure is, however, stable only in very high Ca^{2+} concentrations and without ATP present and must be considered an uncoupled state.

Mutational studies propose that Ca^{2+} ions enter through a single pathway to the two cooperative binding sites (sites I and II): the first Ca^{2+} ion gains access to site I through site II with Glu^{309} as a gating residue, and conformational changes induced by the Ca^{2+} occupation of site I stimulate high affinity binding at site II (21). To do so, the ions would follow a pathway between M1, M2, and M4: the N-path (Fig. 1*a*) (22, 23). The following transfer of the γ-phosphate from bound ATP to Asp^{351} is associated with closure of the N-path and occlusion of the Ca^{2+} ions by formation of a hydrophobic cluster of amino acid residues of M1 and M2, blocking entry to the Ca^{2+} sites (13, 24, 25). In NKA, Glu^{329} is equivalent to SERCA Glu^{309} and plays a similar role in ion gating (26). The plasma membrane and secretory pathway Ca^{2+}-ATPases (PMCAs and SPCAs) both lack an acidic residue in site I, which is consistent with the binding and transport of only one Ca^{2+} ion per hydrolyzed ATP (27, 28).

In support of the N-path for Ca^{2+} binding, crystal structures of SERCA in complex with the inhibitors cyclopiazonic acid and 2,5-di-*tert*-butylhydroquinone, which interfere with Ca^{2+} binding, reveal an inhibitor-binding cleft at the lipid interface between the kinked M1 and M2-M4. (29–32). A divalent cation bound between cyclopiazonic acid and SERCA further hinted at a transient Ca^{2+} site located at the entry to the N-path (29). In further accordance with the N-path, molecular dynamics (MD) simulations of SERCA show a water-filled cytoplasmic pathway toward Glu^{309} and a local negative potential that attracts positively charged ions *in silico* (33). Moreover, the analogous N-path in NKA was pinpointed as the Na^+ entry pathway by cysteine scanning experiments on palytoxin-inhibited enzyme (34). Confirming this model, a recent SERCA structure trapped in a Ca^{2+}-free *E*1 state (in complex with the regulatory protein sarcolipin) is in evident agreement with such a cytoplasmic path leading to Glu^{309} at the ion-binding sites (35). The *E*1 pathway is stabilized by Mg^{2+} ions with the ion-binding sites in seemingly deprotonated states, in remarkable analogy to the luminal pathway of the *E*2P structure, and hints at Mg^{2+} modulation of Ca^{2+} binding. Recently, the Cu^+-ATPase structure also pointed to an N-path, however further functionalized by an N-terminal platform consisting of P_{IB}-specific helices MA and MB (36).

Cytoplasmic Pathway II: The "C-path" in NKA

The C-terminal region of NKA was found to be important for ion binding in binding kinetics studies (3). The structure shows that the C-terminal tyrosine of the α-subunit forms a plug at the cytoplasmic end of a cavity lined by several polar and charged residues between helices M5, M7, M8, and M10 connected to the ion-binding sites (Fig. 1*b*). Electrophysiological studies suggest that the cavity forms an ion pathway (37). Neither of the NKA crystal structures (3, 38) reveals water molecules in this region, but MD simulations suggest that the release of the C-terminal plug or its destabilization by mutation will allow water molecules to enter this cavity (37). Furthermore, electrophysiological studies indicate that during the enzymatic cycle, a proton enters and leaves via the C-terminal region to neutralize one of the three Na^+-binding sites (at Asp^{930} for the human α2-isoform) when the two K^+ ions are countertransported (37). Mutations in the C-terminal end of the α-subunit, as well as in residues lining the cavity, are associated with neurological disorders referred to as familial hemiplegic migraine 2 and rapid-onset dystonia parkinsonism (39, 40), underlining that the cavity is important for proper pump function.

A C-path Also in SERCA1a?

The four C-terminal helices (M7–M10) that form the cavity against M5 in NKA are a shared characteristic of the P_{II} subfamily of P-type ATPases. In SERCA1a, the region is highly hydrophilic (Asp^{981}, Asn^{911}, Asn^{914}, Gln^{759}, Ser^{766}, Ser^{767}, Tyr^{837}, and Arg^{836}), and in a recent 2.2 Å crystal structure of SERCA1a in the AlF_4^--bound transition state of *E*2-P dephosphorylation, a number of well defined, bound water molecules are revealed inside this narrow elongated cavity (C-path; Protein Data Bank code 3N5K) (Fig. 1, *a–d*). The cavity extends from the cytoplasmic interface to the ion-coordinating residues (Asn^{768}, Glu^{771}, Asn^{796}, Asp^{800}, and Glu^{908}), and therefore, it could form a direct ion exit pathway. Three water molecules occupy the Ca^{2+}/H^+-binding sites surrounded by Glu^{309}, Ser^{767}, Asn^{768}, Glu^{771}, Asn^{796}, Asp^{800}, and Glu^{908}, and another six form a "hydration path" between M5, M6, M7, M8, and M10 leading to the cytoplasmic solvent side (Fig. 1, *b–d*). Seven of the nine water molecules in the cleft are visible in both molecules of the asymmetric unit of the 2.2 Å structure and have in part also been observed in other thapsigargin-bound crystal forms of SERCA1a (17, 31, 41).

In contrast to NKA, SERCA lacks the C-terminal "plug" to seal the cavity from cytoplasmic solvent, but two pairs of charged residues (Arg^{762}-Glu^{918} and Arg^{836}-Asp^{981}) located at the cytoplasmic end of the C-path in SERCA would be obvious candidates to function as access gates by formation or release of ionic interactions in a state-dependent manner. The involvement of water molecules in SERCA function has not been investigated in much detail, but MD simulations of SERCA1a in the *E*2 state confirm a continuous water path through the C-terminal pathway, stretching from Glu^{908} of the ion-binding site to Asp^{813} of the L6-L7 loop (Refs. 33 and 42 and further analyses of simulations herein).

The residue that corresponds to the proton-shuttling Asp^{930} in NKA is a conserved asparagine in Ca^{2+}-ATPases (SERCA1a Asn^{911}), which provides a hydrogen bond donor/acceptor rather than a titratable acidic group. This might reflect the different functions: proton shuttling in the control of a unique site III in NKA *versus* unidirectional proton release via a water chain in SERCA. Asn^{911} at a strategic position might in fact be able to function as a switch: paving a water-mediated proton wire by coordination of water molecules or blocking proton transfer if inserted into the pathway.

The C-path Changes with the Functional Cycle of SERCA

Comparing the structural details of this region in all available SERCA1a conformations reveals a clear internal cavity in all *E*2-like (*i.e.* Ca^{2+}-free) states, between M5, M7, M8, and M10, whereas the cavity is absent or negligibly small in Ca^{2+}-bound *E*1 states (Fig. 2). The same effect is observed in MD simulations of SERCA in different states (Refs. 33 and 42 and further analyses of simulations herein).

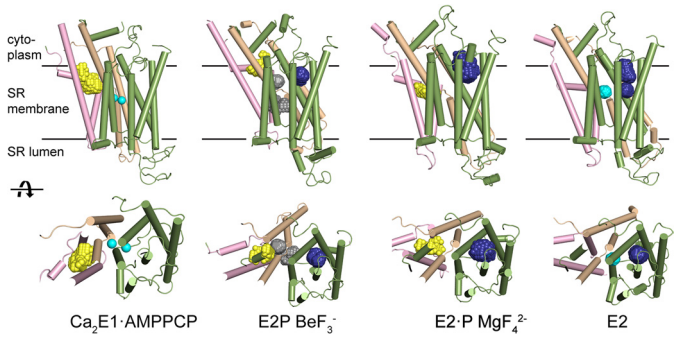

FIGURE 2. **TM section and cavities of SERCA1a in different catalytic states.** A C-terminal cavity (*blue*) is present in all *E*2-like states between TM helices M5, M7, M8, and M10 (color-coded numbering; see the color code described in the legend to Fig. 1). In the *E*2 states, the cavity is enlarged and can contain tightly coordinated water molecules. Structural representations are as follows: Ca_2E1-AMPPCP, Protein Data Bank code 1T5S (13); *E*2P BeF_3^-, code 3B9B (16); *E*2·P MgF_4^{2-}, code 3FGO (29); and *E*2, code 3NAL (57). Cavities and clefts were analyzed with the program McVol (58). For clarity, only cavities in the relevant protein region and large enough to engulf at least one water molecule are shown. Sporadic small cavities, which are present in both *E*1 and *E*2 states, were also omitted for clarity. The coordinates for 1T5S were re-refined and re-deposited (new Protein Data Bank code 3N8G) in the course of this analysis, updating the assignment of a Ca^{2+} *versus* a Mg^{2+} ion coordinated at the nucleotide-binding site, in light of consecutive findings (59). *SR*, sarcoplasmic reticulum.

The helix movements within the cavity-enclosing bundle are subtle but significant. During the *E*1P-to-*E*2P transition, the cytoplasm-facing termini of M5 and M7 tilt slightly away from each other (with the movement of M5 being induced by its insertion into the moving P-domain), opening the cavity for water influx. The three water molecules at the ion-binding sites most probably enter through the luminal pathway along with the protons that neutralize the negatively charged residues after Ca^{2+} release, but the opening of a C-terminal cleft in the *E*2 states suggests that the other water molecules in the C-path come from the cytoplasmic side.

Mutations Affecting the C-path

Several disease-causing mutations that map to the C-path significantly impair the function of NKA (37, 43, 44). In SERCA, mutational studies similarly show the region to be important for function. The R762I mutant has a reduced rate of $[H_n]E2$ to $[Ca_2]E1$ transition (45), and mutation of Ser^{766} (to Cys, Val, or Leu) strongly reduces the apparent Ca^{2+} affinity and ATPase activity (46–48). Strikingly, in SERCA2b, mutations analogous to S766L and E918K in SERCA1a (situated at critical positions at either end of the channel/cavity) cause Darier disease, a genetic skin disorder (47, 49). Milder but measurable effects are furthermore observed for Q759A (45, 48, 50) and N914A (48, 50). Various mutations of Tyr^{763} slow down SERCA activity (48), whereas removal of the side chain in Y763G causes uncoupling (ATP hydrolysis without Ca^{2+} transport) (51). From the structures, it is evident that without the bulky tyrosine side chain, an extra cavity in immediate vicinity to the Ca^{2+}-binding sites would appear. This would possibly allow Ca^{2+} or protons to leak through the C-terminal pathway during the *E*1P-to-*E*2P transition when the C-path reforms. These studies provide further support for a functional role of the C-path in SERCA.

What Is the Functional Role of the C-path?

Previously, the possible hydration of the ion pathways in the P-type ATPases had been scarcely addressed. Notably, a structure-based *in silico* analysis of SERCA (15) has proposed that rapid proton binding from the luminal side depends on chains of water molecules. It was suggested that there are two separate hydrated pathways on the luminal side, one for the exit of Ca^{2+} and one for the entry of H^+. The advantages of the ions following separate routes include that they avoid having to share a single access channel, and the vacated (*i.e.* highly unstable (42)) binding sites may be neutralized simultaneously. Karjalainen *et al.* (15) also obtained evidence for extensive entry of water molecules into the same C-path, where we now present solid crystallographic evidence of bound waters. However, although the authors suggested the use of bifurcated ion pathways on the luminal side, they argued against ions passing through the C-path, primarily because of the positively charged Lys^{758}, Lys^{985}, Arg^{762}, and Arg^{836}, which would prevent cations from passing. The exit of protons would, however, probably not be significantly hindered by these basic residues. In fact, during the catalytic cycle, the estimated pK_a of Lys^{758} and Lys^{985} may fluctuate around 7–8 (52), making them titratable and thereby suitable stepping stones for protons leaving the ion-binding sites or functioning as modulators of nearby carboxylic acid residues for proton hopping.

As noted above, for NKA, a cytoplasmic proton was suggested to shuttle to and from Asp^{930} (human α2 numbering) via the C-path, but it has not been shown so far whether any of the transported Na^+ or K^+ ions also use the pathway. At present, it seems most likely that in both NKA and SERCA, the C-terminal helices have evolved as separate proton pathways, coupled with the ATPase driven cycle. We anticipate that a C-terminal pathway is also functionally adapted in the plasma membrane Ca^{2+}-ATPases, SPCAs, and H^+/K^+-ATPases.

It should be mentioned at this point that the $[H_n]E2$-to-$[Ca_2]E1P$ transition in SERCA is greatly accelerated by high pH, indicating that the rate of *E*1 formation from *E*2 is dependent on release of H^+ before Ca^{2+} can bind (53). At the same time, in SPCA, in which no countertransport of H^+ has been observed, the breakdown of *E*2 phosphoenzyme is not pH-dependent (28).

Earlier studies of the cytoplasmic loop between M6 and M7 have indicated its importance for the functional properties of the ATPase. The loop is situated right above the C-path opening and contains several charged residues (Asp^{813}, Asp^{815}, and Asp^{818}) near the lipid-water interface, and it was suggested to be involved in Ca^{2+} binding (54). However, it seems that the lower apparent Ca^{2+} affinity of an L6-L7 loop mutant observed during ATP hydrolysis may be caused by an impaired rewinding of M6 into the Ca^{2+}-binding conformation (55) or a mere loss of proton-abstracting capacity, thus favoring the protonated state and decelerating deprotonation.

Bifurcated pathways may be specific for the P_{II}-type ATPases because of the strong cooperativity of transport and countertransport. Structures are known for members of two other subfamilies, namely the proton pump AHA2 (subfamily P_{III}), which transports ions one way, and the heavy metal pump

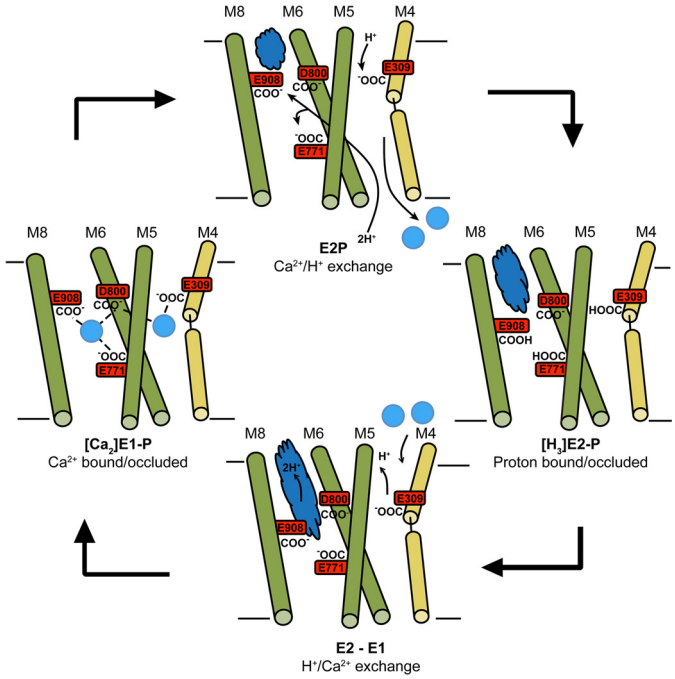

FIGURE 3. **Schematic model for events in the Ca^{2+} ion-binding sites and the ion pathways during the functional cycle of SERCA.** The four TM helices contributing to the binding sites are shown as *rods*, with M4 in *yellow* and M5, M6, and M8 in *green*. Ca^{2+} ions are shown as *cyan spheres*, and Ca^{2+} ion coordinations are indicated by *dashed lines* in the Ca^{2+}-bound *E*1 state, with Asp^{800} coordinating both of the ions. The protonation states of the four acidic residues framing the Ca^{2+} ion-binding sites are highlighted. As the functional cycle of SERCA is fully reversible, the *arrows* could in principle be reversed.

CopA (subfamily P_I), which lacks the C-terminal helix bundle and in which countertransport also is not expected (53). In the proton pump, compensation of the single charged proton-binding residue in the TM region appears to be achieved by an unusually large, hydrated cavity (56), whereas the copper pump features uncharged cysteines in the TM part (36) (although deprotonation/protonation of cysteines may also be associated with copper transport). We thus speculate that the introduction of two ion gateways on both sides of the membrane for coupled exit and entry of ions provides an efficient mechanism for the coordination of transport and countertransport processes.

Concluding Remarks

We find that a C-terminal hydrated proton path in the TM region of SERCA correlates well with all of the observations discussed above and should therefore be considered in future studies on countertransport mechanisms of SERCA and related pumps. Based on the points raised here, a tentative scheme for the ion exchange events in the functional cycle of SERCA is presented in Fig. 3. Starting from the occluded Ca^{2+}-bound $[Ca_2]E1P$ state, the protein is phosphorylated during the transition to the *E*2P state, and Ca^{2+} ions are released to the sarcoplasmic reticulum. As suggested by Musgaard *et al.* (42), one proton may bind through the N-path from the cytoplasmic side, whereas two protons bind from the luminal side, potentially through the luminal proton pathway suggested by Karjalainen *et al.* (15). At the same time, the C-path starts forming. SERCA then enters a proton-occluded state ($[H_3]E2$-P) before the $[H_3]E2$-to-*E*1 transition occurs. During this transition, one proton may be released to the cytoplasm through the N-path (42), whereas the other two are released through the open C-path more or less simultaneously with Ca^{2+} binding through the N-path in formation of the $[Ca_2]E1$-ATP state. The C-path and the N-path then close, coupled with phosphorylation, and the occluded $[Ca_2]E1P$ state is regenerated. This mechanism illustrates a possible way in which a smooth exchange of protons and Ca^{2+} ions can occur and is in accordance with the present structural and functional data.

Acknowledgments—We thank Dr. Laure Yatime for help with data collection and Prof. Marc le Maire for valuable discussions on C-terminal pathways in SERCA. We are grateful for beam time obtained at the Swiss Light Source (Villigen, Switzerland), EMBL-DESY (Hamburg, Germany), and MAX-lab (Lund, Sweden).

REFERENCES

1. Andersen, J. P., and Vilsen, B. (1995) Structure-function relationships of cation translocation by Ca^{2+}- and Na^+,K^+-ATPases studied by site-directed mutagenesis. *FEBS Lett.* **359,** 101–106
2. Clarke, D. M., Loo, T. W., Inesi, G., and MacLennan, D. H. (1989) Location of high affinity Ca^{2+}-binding sites within the predicted transmembrane domain of the sarcoplasmic reticulum Ca^{2+}-ATPase. *Nature* **339,** 476–478
3. Morth, J. P., Pedersen, B. P., Toustrup-Jensen, M. S., Sørensen, T. L., Petersen, J., Andersen, J. P., Vilsen, B., and Nissen, P. (2007) Crystal structure of the sodium-potassium pump. *Nature* **450,** 1043–1049
4. Toyoshima, C., Nakasako, M., Nomura, H., and Ogawa, H. (2000) Crystal structure of the calcium pump of sarcoplasmic reticulum at 2.6 Å resolution. *Nature* **405,** 647–655
5. Strock, C., Cavagna, M., Peiffer, W. E., Sumbilla, C., Lewis, D., and Inesi, G. (1998) Direct demonstration of Ca^{2+} binding defects in sarco-endoplasmic reticulum Ca^{2+}-ATPase mutants overexpressed in COS-1 cells transfected with adenovirus vectors. *J. Biol. Chem.* **273,** 15104–15109
6. Jardetzky, O. (1966) Simple allosteric model for membrane pumps. *Nature* **211,** 969–970
7. Läuger, P. (1979) A channel mechanism for electrogenic ion pumps. *Biochim. Biophys. Acta* **552,** 143–161
8. Vidaver, G. A. (1966) Inhibition of parallel flux and augmentation of counter flux shown by transport models not involving a mobile carrier. *J. Theor. Biol.* **10,** 301–306
9. Albers, R. W. (1967) Biochemical aspects of active transport. *Annu. Rev. Biochem.* **36,** 727–756
10. Post, R. L., Kume, S., Tobin, T., Orcutt, B., and Sen, A. K. (1969) Flexibility of an active center in sodium-plus-potassium adenosine triphosphatase. *J. Gen. Physiol.* **54,** 306–326
11. de Meis, L., and Vianna, A. L. (1979) Energy interconversion by the Ca^{2+}-dependent ATPase of the sarcoplasmic reticulum. *Annu. Rev. Biochem.* **48,** 275–292
12. Jencks, W. P. (1989) How does a calcium pump pump calcium? *J. Biol. Chem.* **264,** 18855–18858
13. Sørensen, T. L., Møller, J. V., and Nissen, P. (2004) Phosphoryl transfer and calcium ion occlusion in the calcium pump. *Science* **304,** 1672–1675
14. Olesen, C., Sørensen, T. L., Nielsen, R. C., Møller, J. V., and Nissen, P. (2004) Dephosphorylation of the calcium pump coupled to counterion occlusion. *Science* **306,** 2251–2255
15. Karjalainen, E. L., Hauser, K., and Barth, A. (2007) Proton paths in the sarcoplasmic reticulum Ca^{2+}-ATPase. *Biochim. Biophys. Acta* **1767,** 1310–1318
16. Olesen, C., Picard, M., Winther, A. M., Gyrup, C., Morth, J. P., Oxvig, C., Møller, J. V., and Nissen, P. (2007) The structural basis of calcium transport by the calcium pump. *Nature* **450,** 1036–1042
17. Toyoshima, C., Norimatsu, Y., Iwasawa, S., Tsuda, T., and Ogawa, H.

(2007) How processing of aspartylphosphate is coupled to lumenal gating of the ion pathway in the calcium pump. *Proc. Natl. Acad. Sci. U.S.A.* **104,** 19831–19836
18. Clausen, J. D., and Andersen, J. P. (2010) Glutamate 90 at the luminal ion gate of sarcoplasmic reticulum Ca^{2+}-ATPase is critical for Ca^{2+} binding on both sides of the membrane. *J. Biol. Chem.* **285,** 20780–20792
19. Yatime, L., Laursen, M., Morth, J. P., Esmann, M., Nissen, P., and Fedosova, N. U. (2011) Structural insights into the high affinity binding of cardiotonic steroids to the Na^+,K^+-ATPase. *J. Struct. Biol.* **174,** 296–306
20. Bishop, J. E., and Al-Shawi, M. K. (1988) Inhibition of sarcoplasmic reticulum Ca^{2+}-ATPase by Mg^{2+} at high pH. *J. Biol. Chem.* **263,** 1886–1892
21. Inesi, G., Ma, H., Lewis, D., and Xu, C. (2004) Ca^{2+} occlusion and gating function of Glu^{309} in the ADP-fluoroaluminate analog of the Ca^{2+}-ATPase phosphoenzyme intermediate. *J. Biol. Chem.* **279,** 31629–31637
22. Toyoshima, C., and Nomura, H. (2002) Structural changes in the calcium pump accompanying the dissociation of calcium. *Nature* **418,** 605–611
23. Jensen, A. M., Sørensen, T. L., Olesen, C., Møller, J. V., and Nissen, P. (2006) Modulatory and catalytic modes of ATP binding by the calcium pump. *EMBO J.* **25,** 2305–2314
24. Toyoshima, C., and Mizutani, T. (2004) Crystal structure of the calcium pump with a bound ATP analogue. *Nature* **430,** 529–535
25. Inesi, G., Kurzmack, M., Coan, C., and Lewis, D. E. (1980) Cooperative calcium binding and ATPase activation in sarcoplasmic reticulum vesicles. *J. Biol. Chem.* **255,** 3025–3031
26. Einholm, A. P., Andersen, J. P., and Vilsen, B. (2007) Roles of transmembrane segment M1 of Na^+,K^+-ATPase and Ca^{2+}-ATPase, the gatekeeper and the pivot. *Bioenerg. Biomembr.* **39,** 357–366
27. Clark, A., and Carafoli, E. (1983) The stoichiometry of the Ca^{2+}-pumping ATPase of erythrocytes. *Cell Calcium* **4,** 83–88
28. Dode, L., Andersen, J. P., Raeymaekers, L., Missiaen, L., Vilsen, B., and Wuytack, F. (2005) Functional comparison between secretory pathway Ca^{2+}/Mn^{2+}-ATPase (SPCA) 1 and sarcoplasmic reticulum ATPase (SERCA) 1 isoforms by steady-state and transient kinetic analyses. *J. Biol. Chem.* **280,** 39124–39134
29. Laursen, M., Bublitz, M., Moncoq, K., Olesen, C., Møller, J. V., Young, H. S., Nissen, P., and Morth, J. P. (2009) Cyclopiazonic acid is complexed to a divalent metal ion when bound to the sarcoplasmic reticulum Ca^{2+}-ATPase. *J. Biol. Chem.* **284,** 13513–13518
30. Moncoq, K., Trieber, C. A., and Young, H. S. (2007) The molecular basis for cyclopiazonic acid inhibition of the sarcoplasmic reticulum calcium pump. *J. Biol. Chem.* **282,** 9748–9757
31. Obara, K., Miyashita, N., Xu, C., Toyoshima, I., Sugita, Y., Inesi, G., and Toyoshima, C. (2005) Structural role of countertransport revealed in Ca^{2+} pump crystal structure in the absence of Ca^{2+}. *Proc. Natl. Acad. Sci. U.S.A.* **102,** 14489–14496
32. Takahashi, M., Kondou, Y., and Toyoshima, C. (2007) Interdomain communication in calcium pump as revealed in the crystal structures with transmembrane inhibitors. *Proc. Natl. Acad. Sci. U.S.A.* **104,** 5800–5805
33. Musgaard, M., Thøgersen, L., Schiøtt, B., and Tajkhorshid, E. (2012) Tracing cytoplasmic Ca^{2+} ion and water access points in the Ca^{2+}-ATPase. *Biophys. J.* **102,** 268–277
34. Takeuchi, A., Reyes, N., Artigas, P., and Gadsby, D. C. (2008) The ion pathway through the opened Na^+,K^+-ATPase pump. *Nature* **456,** 413–416
35. Winther, A. M. L., Bublitz, M., Karlsen, J. L., Møller, J. V., Hansen, J. B., Nissen, P., Buch-Pedersen, M. J. (2013) The sarcolipin-bound calcium pump stabilizes calcium sites exposed to the cytoplasm. *Nature*, **495,** 265–269
36. Gourdon, P., Liu, X. Y., Skjørringe, T., Morth, J. P., Møller, L. B., Pedersen, B. P., and Nissen, P. (2011) Crystal structure of a copper-transporting PIB-type ATPase. *Nature* **475,** 59–64
37. Poulsen, H., Khandelia, H., Morth, J. P., Bublitz, M., Mouritsen, O. G., Egebjerg, J., and Nissen, P. (2010) Neurological disease mutations compromise a C-terminal ion pathway in the Na^+/K^+-ATPase. *Nature* **467,** 99–102
38. Shinoda, T., Ogawa, H., Cornelius, F., and Toyoshima, C. (2009) Crystal structure of the sodium-potassium pump at 2.4 Å resolution. *Nature* **459,** 446–450
39. de Carvalho Aguiar, P., Sweadner, K. J., Penniston, J. T., Zaremba, J., Liu, L., Caton, M., Linazasoro, G., Borg, M., Tijssen, M. A., Bressman, S. B., Dobyns, W. B., Brashear, A., and Ozelius, L.J. (2004) Mutations in the Na^+/K^+-ATPase α3 gene *ATP1A3* are associated with rapid-onset dystonia parkinsonism. *Neuron* **43,** 169–175
40. De Fusco, M., Marconi, R., Silvestri, L., Atorino, L., Rampoldi, L., Morgante, L., Ballabio, A., Aridon, P., and Casari, G. (2003) Haploinsufficiency of *ATP1A2* encoding the Na^+/K^+ pump α2 subunit associated with familial hemiplegic migraine type 2. *Nat. Genet.* **33,** 192–196
41. Toyoshima, C., Yonekura, S., Tsueda, J., and Iwasawa, S. (2011) Trinitrophenyl derivatives bind differently from parent adenine nucleotides to Ca^{2+}-ATPase in the absence of Ca^{2+}. *Proc. Natl. Acad. Sci. U.S.A.* **108,** 1833–1838
42. Musgaard, M., Thøgersen, L., and Schiøtt, B. (2011) Protonation states of important acidic residues in the central Ca^{2+} ion binding sites of the Ca^{2+}-ATPase: a molecular modeling study. *Biochemistry* **50,** 11109–11120
43. Morth, J. P., Poulsen, H., Toustrup-Jensen, M. S., Schack, V. R., Egebjerg, J., Andersen, J. P., Vilsen, B., and Nissen, P. (2009) The structure of the Na^+,K^+-ATPase and mapping of isoform differences and disease-related mutations. *Philos. Trans. R. Soc. Lond. B Biol. Sci.* **364,** 217–227
44. Toustrup-Jensen, M. S., Holm, R., Einholm, A. P., Schack, V. R., Morth, J. P., Nissen, P., Andersen, J. P., and Vilsen, B. (2009) The C terminus of Na^+,K^+-ATPase controls Na^+ affinity on both sides of the membrane through Arg^{935}. *J. Biol. Chem.* **284,** 18715–18725
45. Sørensen, T. L., and Andersen, J. P. (2000) Importance of stalk segment S5 for intramolecular communication in the sarcoplasmic reticulum Ca^{2+}-ATPase. *J. Biol. Chem.* **275,** 28954–28961
46. Clarke, D. M., Loo, T. W., and MacLennan, D. H. (1990) Functional consequences of alterations to polar amino acids located in the transmembrane domain of the Ca^{2+}-ATPase of sarcoplasmic reticulum. *J. Biol. Chem.* **265,** 6262–6267
47. Miyauchi, Y., Daiho, T., Yamasaki, K., Takahashi, H., Ishida-Yamamoto, A., Danko, S., Suzuki, H., and Iizuka, H. (2006) Comprehensive analysis of expression and function of 51 sarco(endo)plasmic reticulum Ca^{2+}-ATPase mutants associated with Darier disease. *J. Biol. Chem.* **281,** 22882–22895
48. Rice, W. J., and MacLennan, D. H. (1996) Scanning mutagenesis reveals a similar pattern of mutation sensitivity in transmembrane sequences M4, M5, and M6, but not in M8, of the Ca^{2+}-ATPase of sarcoplasmic reticulum (SERCA1a). *J. Biol. Chem.* **271,** 31412–31419
49. Ikeda, S., Mayuzumi, N., Shigihara, T., Epstein, E. H., Jr., Goldsmith, L. A., and Ogawa, H. (2003) Mutations in *ATP2A2* in patients with Darier's disease. *J. Invest. Dermatol.* **121,** 475–477
50. Asahi, M., Kimura, Y., Kurzydlowski, K., Tada, M., and MacLennan, D. H. (1999) Transmembrane helix M6 in sarco(endo)plasmic reticulum Ca^{2+}-ATPase forms a functional interaction site with phospholamban. Evidence for physical interactions at other sites. *J. Biol. Chem.* **274,** 32855–32862
51. Andersen, J. P. (1995) Functional consequences of alterations to amino acids at the M5S5 boundary of the Ca^{2+}-ATPase of sarcoplasmic reticulum. Mutation $Tyr^{763} \rightarrow$ Gly uncouples ATP hydrolysis from Ca^{2+} transport. *J. Biol. Chem.* **270,** 908–914
52. Bas, D. C., Rogers, D. M., and Jensen, J. H. (2008) Very fast prediction and rationalization of pK_a values for protein-ligand complexes. *Proteins* **73,** 765–783
53. Lewis, D., Pilankatta, R., Inesi, G., Bartolommei, G., Moncelli, M. R., and Tadini-Buoninsegni, F. (2012) Distinctive features of catalytic and transport mechanisms in mammalian sarco-endoplasmic reticulum Ca^{2+}-ATPase (SERCA) and Cu^+ (ATP7A/B)-ATPases. *J. Biol. Chem.* **287,** 32717–32727
54. Menguy, T., Corre, F., Juul, B., Bouneau, L., Lafitte, D., Derrick, P. J., Sharma, P. S., Falson, P., Levine, B. A., Møller, J. V., and le Maire, M. (2002) Involvement of the cytoplasmic loop L6–7 in the entry mechanism for transport of Ca^{2+} through the sarcoplasmic reticulum Ca^{2+}-ATPase. *J. Biol. Chem.* **277,** 13016–13028
55. Lenoir, G., Picard, M., Møller, J. V., le Maire, M., Champeil, P., and Falson, P. (2004) Involvement of the L6–7 loop in SERCA1a Ca^{2+}-ATPase acti-

vation by Ca^{2+} (or Sr^{2+}) and ATP. *J. Biol. Chem.* **279,** 32125–32133
56. Pedersen, B. P., Buch-Pedersen M. J., Morth, J. P., Palmgren, M. G., and Nissen, P. (2007) Crystal structure of the plasma membrane proton pump. *Nature* **450,** 1111–1114
57. Winther, A. M., Liu, H., Sonntag, Y., Olesen, C., le Maire, M., Soehoel, H., Olsen, C. E., Christensen, S.B., Nissen, P., and Møller, J.V. (2010) Critical roles of hydrophobicity and orientation of side chains for inactivation of sarcoplasmic reticulum Ca^{2+}-ATPase with thapsigargin and thapsigargin analogs. *J. Biol. Chem.* **285,** 28883–28892
58. Till, M. S., and Ullmann, G. M. (2010) McVol–a program for calculating protein volumes and identifying cavities by a Monte Carlo algorithm. *J. Mol. Model.* **16,** 419–429
59. Picard, M., Jensen, A. M., Sørensen, T. L., Champeil, P., Møller, J. V., and Nissen, P. (2007) Ca^{2+} versus Mg^{2+} coordination at the nucleotide-binding site of the sarcoplasmic reticulum Ca^{2+}-ATPase. *J. Mol. Biol.* **368,** 1–7